Correction for the effects of distance on terrestrial LiDAR intensity data under different illumination conditions

Rahuan Miguel da Silva [1], Antonio Maria Garcia Tommaselli [1], Isabella Subtil Norberto [1], Renato César dos Santos [1]

[1] Department of Cartography, São Paulo State University (UNESP), Presidente Prudente, SP 19060-900, Brazil – (rahuan.miguel, a.tommaselli, isabella.subtil, renato.cesar)@unesp.br

Keywords: Polynomial fitting, Intensity correction, Terrestrial LASER Scanner, Illumination, Range-Based, Distance effect.

1.Introduction

The Light Amplification by Stimulated Emission of Radiation (LASER) scanning systems can acquire high-precision spatial information. They record tridimensional coordinates (x, y, z) and the intensity of the backscattered signal power. However, intensity information is often underused, since the measured values are affected by four main factors: instrumental, atmospheric, target characteristics, and measurement geometry (Kaasalainen et al., 2011).

Corrected intensity can be obtained using different theoretical and empirical models. However, most models only consider geometric factors, such as distance and angle of incidence. After correction, the intensity can be normalised according to a homogeneous reference, turning it into valuable data for various applications, such as target detection and classification, fusion with computer vision, and others..

Having data proportional to reflectance is essential in vegetation studies using LASER systems, which typically operate at infrared wavelengths and are sensitive to the physiological state of leaves and water stress. In this context, we can mention applications involving forest inventory and agricultural automation, where productivity can be estimated by detecting fruit and identifying diseased plants using the intensity corrected derived from point cloud.

In this study, we propose correcting the intensity using a polynomial fit with data from targets collected at various distances. For that, the experiments were conducted using two study areas in different environments (indoor and outdoor) to evaluate the impact of lighting variation on FARO Focus Premium measurements.

The construction of the proposed polynomial correction model requires an experimental design that allows the effect of distance on the measured intensity to be isolated. To this end, it is essential to use targets that are representative of the object under study and, at the same time, provide a stable reference. Thus, this work uses a multi-target approach.

To further investigate the response to the water content of plants, we selected healthy, dry leaves as targets of interest. Artificial targets were also used, providing targets whose radiometric characteristics do not change, thus enabling radiometric calibration of intensity data in the future.

The artificial targets selected were white and black EVA foam, which were used as a reference for model adjustment, allowing the intensity values to be normalised at the end of the process.

2. Method

The processing flow carried out for this study can be divided into four parts: data acquisition, pre-processing, intensity correction, and finally, evaluation of the quality of the results. Figure 1 shows the flowchart of the processes performed.

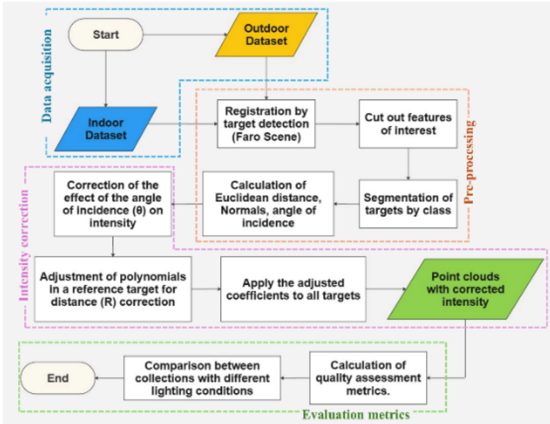

Figure 1. Flowchart of the processes performed.

2.1 Data acquisition

The instrument used for data acquisition was the FARO Focus Premium terrestrial LASER scanner (TLS), a high-resolution system capable of generating detailed three-dimensional point clouds. Designed to produce data with millimetre accuracy, it includes automatic scan registration and integration with processing software. Table 1 presents the technical specifications of the FARO Focus Premium.

Specifications	FARO Focus Premium 70
Wavelength	1553.5 nm
Max. Range	350 m (White targets) 150 m (Dark targets)
Beam divergence	0.3 mrad (0.024°)(1/e)
Beam exit diameter	2.12 mm (1/e)
Field of view	360° × 300°

Table 1. LiDAR Specifications. Source: Adapted from FARO User Manual (2022).

In order to evaluate the impact of sunlight on the data collected by an active sensor and the behaviour of the materials , this study employed two datasets with distinct lighting conditions. Both datasets were collected at the Sao Paulo State University (UNESP) campus, Presidente Prudente, São Paulo.

As the objective of the research is to adjust the intensity so that it is not influenced by distance, this variation between the sets does not affect the analysis. The reference distance serves as a common data for adjustment between the two experiments.

The first dataset was collected outdoors and during the afternoon between 1:30 and 3:00 p.m.. The calibration panel was oriented perpendicular to geographic north, using local coordinates. Scan positions were carefully marked with ground control points to ensure accurate distances between the scanner and the panel. For this outdoor dataset, the distances were set to 1.5 m, 3 m, 4.5 m, 9 m, and 12 m (Figure 2). The second dataset was collected indoors at night to eliminate sunlight interference. In this case, the scan positions were set at 2 m, 3 m, 4 m, 5 m, 10 m, and 15 m (Figure 2). In both datasets, the sensor was oriented perpendicular to the plate, resulting in an angle of incidence close to zero.

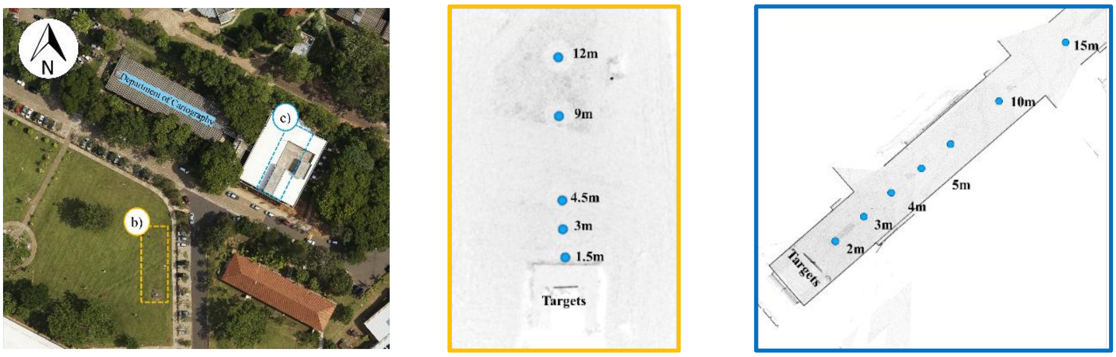

(a) (b) (c)

Figure 2: Data acquisition for outdoor (yellow rectangle) and indoor (blue rectangle) environments (a). LiDAR stations for outdoor collection (b); and indoor collection (c). Blue circles represent the stations.

Figure 2 shows the spatial arrangement of scan positions relative to the panel for both datasets. Each dataset maintained the same set of leaf types; each healthy leaf was paired with its dry counterpart on the same panel.

In data collection, various types of targets were placed on a wooden board (Figure 3). This board is referred to as the 'calibration panel' throughout the text. This panel contained 43 targets, including six EVA samples, three sandpapers, four tree barks, four fruit peels, and 26 leaves (thirteen healthy and thirteen dry).

Figure 3 highlights the selected targets (rectangle with yellow dashed outline) for each dataset. For this representation, the external and internal collections chosen were the 3 m stations, as this is the reference distance.

Id	Selected targets
01	Black EVA (Smooth side)
02	White EVA (Smooth side)
03	Healthy leaf 1
04	Dry leaf 1
05	Healthy leaf 2
06	Dry leaf 2
07	Healthy leaf 3
08	Dry leaf 3
09	Healthy leaf 4
10	Dry leaf 4

Figure 3. The targets selected for data processing (numbered from 01 to 10).

For nighttime indoor acquisition, healthy leaves were replaced due to natural senescence, since the data were collected on different days. This replacement was necessary because leaf senescence significantly affects the recorded intensity values.

2.2 Pre-processing

After data collection, all scans from different distances were registered using the FARO Focus integrated software. The registration process relied on spherical target detection and least squares adjustment of a rigid body transformation.

From the aligned point clouds, ten (10) targets were selected and classified for analysis in this study: two EVA plates (white and black), four healthy leaves, and four dry leaves. These targets were chosen to investigate the intensity response of leaves under different hydration conditions.

2.3 Intensity correction

Intensity correction is a challenging topic due to a lack of standardisation. In this sense,raises the issue different terminologies are used (Kashani et al., 2015). Several empirical models applied to TLS systems are found in the literature (Kaasalainen et al., 2011; Carrea et al., 2016). These models suggest that the equation best describing the effects on intensity are derived by adapting RADAR (Radio Detecting and Ranging) concepts and using Wagner's (2010) equation to calculate the backscattered signal power (Equation 1).

$$P_r = \frac{P_t D_r^2}{4\pi R^4 \beta_t^2} \eta_{sys} \eta_{atm} \sigma \tag{1}$$

Where P_r is the received signal power in watts, R is the range in meters, β_t is the beam width in radians, and D_r is the detector aperture in meters. η_{sys} is a factor indicating the transmission efficiency of the optical components of the LASER system. Additionally, η_{atm} is the atmospheric transmission factor, and σ is the target's cross-sectional area in square meters.

Assuming the target is larger than the LASER footprint and has a diffuse (Lambertian) surface, the RADAR equation (Equation 1) can be rewritten by considering certain simplifications: (i) the instrumental factors are constant and; (ii) the atmospheric factors are negligible at short distances, under controlled conditions, and when using the same sensor system (Carrea et al., 2016).

Considering that the received power (Equation 1) is proportional to the recorded intensity ($I_{(\rho,\ \theta,\ d)}$), Equation 2 (adapted from Carrea et al., 2016) can be derived:

$$I_{(\rho,\theta,d)} \propto \frac{\rho_\lambda \cos\theta}{R^2} \tag{2}$$

The intensity collected varies depending on the material's properties at the pulse wavelength ($\rho\lambda$), angle of incidence (θ), and distances (d). However, the primary information that we are interested in is the material's properties. Then, it is assumed that the corrected intensity is exclusively governed by the intrinsic properties of the material.

Therefore, the equation is dependent on distance when the plate containing the targets is perpendicular to the sensor and the angle of incidence is nearly zero. Lambert's cosine law establishes that when the angle of incidence is close to zero, the intensity of the energy reflected back to the sensor is maximized, suffering only a minimal reduction for small angular variations (Blaskow & Schneider, 2014).

For points distant from the plate's centre or with reliefs on its surface neighbourhoods, the calculated angles of incidence were greater than 25° at some points. Therefore, considering Lambert's cosine law, the loss caused by the angle is approximately 9.4%, which cannot be considered a negligible factor for these targets.

Given that the intensity is a function of the angle of incidence and distance, it is possible to eliminate points that exceed 15° by applying a simplified correction of the angle of incidence that considers the ratio between the intensity and the cosine of the angle of incidence.

The simplified equation was adopted, considering that all targets were fixed on the same plate. Thus, the variation in the angle of incidence is mainly due to the distance of the LASER beam in relation to the targets and the small irregularities present on the surface of the materials.

For distance correction, a polynomial approximation of the coefficients modelling intensity variation was used. Equation 3 presents the model used in this study, a simplified adaptation of the theoretical model proposed by Bai et al. (2023) to correct for the effects of distance. For the effects of the angle of incidence, Lambert's cosine law adapted from Blaskow and Schneider (2014) was used.

$$I_{(\rho)} = I_{(\rho,\theta,d)} \cdot \frac{\sum_{i=0}^{N=3}(\beta_i d_s^i)}{\sum_{i=0}^{N=3}(\beta_i d^i)} \cdot \frac{1}{\cos(\theta)} \tag{3}$$

For this article, EVA targets are considered as references for correcting the intensity in tree leaves because as artificial targets, they do not undergo significant changes in their radiometric properties, unlike leaves, which undergo senescence a few hours after pruning.

2.4 Evaluation Metrics

Three evaluation metrics were employed to assess the effectiveness of the intensity correction under varying illumination conditions and distances: Root Mean Square Error (RMSE), the coefficient of determination (R^2) and the Coefficient of Variation (CV).

The RMSE quantifies the root of the average squared magnitude of the difference between the observed and corrected intensity values (Equation 4).

$$\mathrm{RMSE} = \sqrt{\frac{1}{n}\sum_{i=1}^{n}(y_i - \hat{y}_i)^2} \tag{4}$$

where y_i represents the observed intensity, $\hat{y}_i$ the modelled intensity after correction, and n the number of observations.

The coefficient of determination (R^2) was obtained using the polynomial regression function in MATLAB. This coefficient shows the proportion of variance in the intensity values that is explained by the fitted model. Values range from 0 to 1, with higher values denoting a better fit.

Relative dispersion of intensity values was quantified using the CV before and after correction. In the context of TLS data, changes in range-dependent parameters such as λ (reflectance-scaled range R_s) can significantly impact the spread of corrected intensity distributions. However, since the absolute scale of intensity values can vary across acquisitions, the standard deviation alone is not sufficient for fair comparisons. CV (Equation 5) is scale-invariant and therefore, enables effective comparison of dispersion degrees across datasets with different mean intensity levels (Höfle and Norbert, 2007; Jutzi et al., 2009).

$$\mathrm{CV} = \frac{\sigma}{\mu} \tag{5}$$

where σ is the standard deviation and μ the mean of the intensity values. The correction quality is evaluated by the ratio between the CV of the corrected and original intensity datasets, as shown in Equation 6.

$$\varepsilon = \frac{\mathrm{CV_{cor}}}{\mathrm{CV_{ori}}} \tag{6}$$

where $\mathrm{CV_{ori}}$ and $\mathrm{CV_{cor}}$ correspond to the coefficient of variation before and after correction, respectively. Values of $\varepsilon < 1$ indicate a reduction in relative dispersion, suggesting that the correction model was effective in stabilising intensity measurements across varying distances and illumination conditions.

3. Results and Discussion

3.1 Results of Intensity Corrections

TLS systems generate dense point clouds with many applications. These systems generate point clouds in a local three-dimensional (3D) coordinate system of the sensor (x, y, z), which can be georeferenced. In this study, the origin of the reference system was the scan at the farthest distance.

Initially, the distances, surface normals, and incidence angles were calculated for all targets in each of the point clouds analysed. Based on these angles, it was possible to identify critical regions in the targets where the incidence angles exceeded 25°.

There are several approaches to mitigate the effects of the angle of incidence, most of which are based on empirical models to estimate calibration parameters. However, a simplified theoretical model based on Lambert's cosine law was implemented, as the variations in the angle of incidence were caused by small inconsistencies in the leaves.

For the application of the correction, white EVA target were selected for the polynomial model fit. Different intensity measurements obtained at various distances for this target were used for the adjustment. In addition, the correction process was conducted using a reference distance of 3 m, as it was the sole common distance between the two sets of data collected and the critical point in the intensity's relationship to distance.

The distances between the scanning station and the targets were referred to as nominal distances, since each point in the cloud has a specific Euclidean distance from the sensor.

Based on the nominal distances and the average intensities of the targets, it was possible to analyse the behaviour of the intensity response at different distances and under varying environmental conditions.

It is important to note that one of the main objectives of this study is to improve the understanding and application of high-precision LiDAR tools for short-range terrestrial applications, with a specific focus on vegetation, particularly in agronomy. Therefore, longer distances were not considered relevant to this research.

Figures 4(a) and (b), illustrate the behaviour of intensity as a function of distance in the two datasets used in this study. There is a clear distinction between healthy leaves and leaves subjected to water stress, with clearly established limits that facilitate the exact identification of the transition between these two situations.

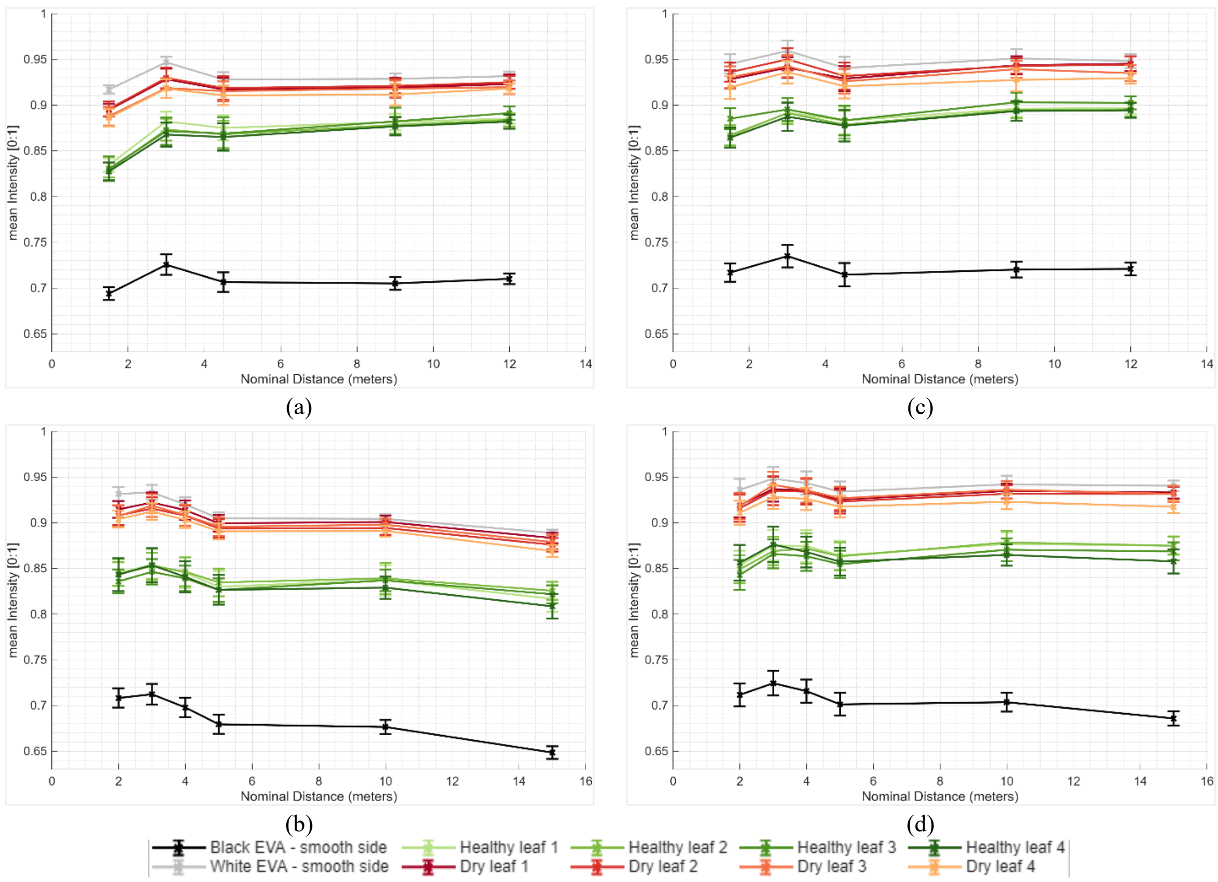

Figure 4. Graph (a) shows the average intensity collected in an outdoor environment in relation to distance; (b) the average intensity collected in an indoor environment in relation to distance; (c) the behaviour of the average intensities collected in an outdoor environment after correction of the effects by the model; and (d) the averages of the intensities collected in an indoor environment after correction of the effects by the model.

Iintensity behaviour observed in the outdoor environment was unexpected (Fugure 4). According to the inverse square law, the reflected energy from an illuminated target should decrease with increasing distance. However, this decrease was not observed; instead, the measured intensity increased as the distance to the sensor increased.

A plausible explanation for this unexpected behavior is that ambient lighting influenced the LASER measurements obtained in the outdoor environment. However, this hypothesis must be further investigated. In addition, it is necessary to eliminate the geometric effects of data acquisition.

A polynomial model was adjusted to correct for the influence of distance. A third-degree polynomial function was chosen based on empirical tests. This selection was performed to determine the degree of the common polynomial that best fits the data without causing overfitting.

Figures 4(c) and 4(d) present the correction of geometric effects. Beyond the graphs in Figure 4, additional metrics (Table 2 and 3, respectively) were computed to allow a more detailed evaluation of the simplified model's quality.

The quantitative evaluation of the intensity correction methodology began with the dataset acquired in an outdoor environment, which represents a realistic collection scenario under the influence of ambient solar radiation. The aim was to evaluate the method under varying lighting conditions by modeling the relationship between intensity and distance.

A coefficient of determination (R^2) of 0.53 was obtained, with a Root Mean Square Error (RMSE) of 0.0062. The moderate value of R^2 suggests that, although distance is a relevant factor, it is not the only source of intensity variation, indicating strong interference from external factors, notably sunlight.

The effectiveness of correcting for the effects of distance was evaluated by analysing the CV. As detailed in Table 2, the methodology proved to be robust, reducing the variability of intensity for all 10 targets. The residual variability, calculated as the ratio between the CV after and before correction, ranged from 38.89% to 68.18%. This result confirms that the correction is successful in mitigating the intensity variations caused by changes in distance and incidence angle, even in the presence of sunlight.

Targets	CV_{ori}	CV_{cor}	ε (%)
Black EVA - smooth side	0.0161	0.011	68.18%
White EVA - smooth side	0.0115	0.0074	64.30%
Healthy leaf 1	0.0242	0.0145	59.81%
Dry leaf 1	0.014	0.0087	62.42%
Healthy leaf 2	0.025	0.0137	54.57%
Dry leaf 2	0.0142	0.0076	53.65%
Healthy leaf 3	0.0268	0.0104	38.89%
Dry leaf 3	0.0148	0.0071	47.99%
Healthy leaf 4	0.0248	0.0142	57.38%
Dry leaf 4	0.0144	0.0074	50.88%

Table 2: Analysis of the Coefficient of Variation (CV) for the Outdoor dataset.

To isolate the effects caused by changes in geometry, to the sunlight influence and establish a baseline performance for the study, the experiment was replicated in a controlled indoor environment. The absence of ambient light resulted in an improvement in the distance effect correction model. The polynomial fit for the reference target achieved an R^2 of 0.94 and an RMSE of 0.0048..

This R^2 demonstrates that, in the absence of external interference, the polynomial model better described the behaviour of intensity in relation to distance. The direct comparison between R^2 of 0.53 (Outdoor) and 0.94 (Indoor) serves as strong quantitative evidence of the disruptive impact of solar radiation on LiDAR intensity measurements.

The CV analysis for the indoor dataset in Table 3, revealed a more pronounced stabilisation of intensity for most targets. The reference target 'White EVA', for example, retains only 28.76% of its original variability.

However, the controlled conditions also allowed us to identify limitations of the model for specific surfaces. The "Healthy leaf 2" and "Healthy leaf 3" targets showed a slight increase in variability after correction, indicating that their reflection properties may diverge from the ideal Lambertian model. This observation, visible only in the controlled environment, underscores the importance of considering material characteristics when applying more robust radiometric correction models.

Targets	CV_ori	CV_cor	ε (%)
Black EVA - smooth side	0.0348	0.0189	54.24%
White EVA - smooth side	0.0191	0.0055	28.76%
Healthy leaf 1	0.0158	0.0107	68.04%
Dry leaf 1	0.0154	0.0075	48.73%
Healthy leaf 2	0.0113	0.0121	106.89%
Dry leaf 2	0.0158	0.0081	50.87%
Healthy leaf 3	0.0107	0.0121	113.50%
Dry leaf 3	0.0152	0.0088	57.63%
Healthy leaf 4	0.0189	0.0091	48.11%
Dry leaf 4	0.017	0.007	41.01%

Table 3: Analysis of the Coefficient of Variation (CV) for the Indoor dataset.

4.Conclusion

The results showed a positive trend in correcting the effects of distance on intensity, reinforcing the methodology's potential for future applications. The fact that the variations were not completely corrected due to the simplified nature of this model highlights the need for more reliable models that take into account material properties and lighting conditions.

Despite these limitations, the intensity data proved promising for use in vegetation analysis, allowing a clear distinction between healthy and dry leaves. These findings highlight the potential of intensity as an indicator of plant water status, especially when the sensor is properly corrected, with applications in areas such as water monitoring and agricultural stress.

The need for more advanced models was demonstrated quantitatively by the comparative analysis between environments. The correction of specific plant targets showed that the reflectance properties of the material are significant and cannot be summarized by a single model. This made the limitations of the simplified method used here even clearer.

The model can be improved by using bidirectional reflectance distribution functions (BRDF) to deal with the complexity of non-Lambertian targets, such as vegetation.

In addition, the intensity of LiDAR needs to be changed from relative data to accurate radiometric measurements in order to make it more advantageous as a quantitative tool for accurately cultivating and monitoring the environment. Therefore, the use of radiometric measurements of reference targets can help model the effects.

Acknowledgements

This study was financed by the São Paulo Research Foundation (FAPESP) – Brazil (grants n. 2021/06029-7), by the Coordenação de Aperfeiçoamento de Pessoal de Nível Superior – Brasil, CAPES (grant n. 88887.961773/2024-0) and by the National Council for Scientific and Technological Development, CNPq (grant n. 303670/2018-5).

References

Bai, J., Niu, Z., Gao, S., Bi, K., Wang, J., Huang, Y., Sun, G., 2023. An exploration, analysis, and correction of the distance effect on terrestrial hyperspectral LiDAR data. ISPRS Journal of Photogrammetry and Remote Sensing 198, 60–83. https://doi.org/10.1016/j.isprsjprs.2023.03.001

Blaskow, R. and Schneider, D., 2014. Analysis and correction of the dependency between LASER scanner intensity values and range, *International Archives of the Photogrammetry, Remote Sensing and Spatial Information Sciences*, **XL–5**, pp. 107–112. https://doi.org/10.5194/isprsarchives-XL-5-107-2014

Carrea, D., Abellán, A., Calvín, J. and Martínez, J., 2016. Correction of terrestrial LiDAR intensity channel using Oren–Nayar reflectance model: An application to lithological differentiation, *ISPRS Journal of Photogrammetry and Remote Sensing*, **113**, pp. 17–29. https://doi.org/10.1016/j.isprsjprs.2015.12.004.

Cheng, X., Cheng, X., Li, Q. & Xu, W., 2018. *LASER intensity correction of terrestrial 3D LASER scanning based on sectional polynomial model*, *LASER & Optoelectronics Progress*, 54(1), 10.3788/LOP54.112802.

FARO Technologies, Inc., 2022. Focus Premium LASER Scanner User Manual. Lake Mary, FL: FARO Technologies, Inc.

HöfLe, B. and Pfeifer, N., 2007. Correction of LASER scanning intensity data: Data and model-driven approaches, *ISPRS Journal of Photogrammetry and Remote Sensing*, **62**(6), pp. 415–433. https://doi.org/10.1016/j.isprsjprs.2007.05.008

Jutzi, Boris, and H. Gross. 2009. Normalisation of LiDAR intensity data based on range and surface incidence angle. *Int. Arch. Photogramm. Remote Sens. Spat. Inf. Sci* 38: 213-218.

Kaasalainen, S., Lindroos, M., Hyyppä, H. and Hyyppä, J., 2011. Analysis of incidence angle and distance effects on terrestrial LASER scanner intensity: Search for correction methods, *Remote Sensing*, **3**(10), pp. 2207–2221. https://doi.org/10.3390/rs3102207

Kashani, A.G., Reutebuch, S.E., McGaughey, R.J. and Oliver, C.D., 2015. A review of LIDAR radiometric processing: From ad hoc intensity correction to rigorous radiometric calibration, *Sensors*, pp. 28099–28128. https://doi.org/10.3390/s151128099

Sanchiz-Viel, N., Marin-Moreno, J.A., Montero, E. and Hernández-López, D., 2021. Radiometric correction of LASER scanning intensity data applied for terrestrial LASER scanning, *ISPRS Journal of Photogrammetry and Remote Sensing*, **172**, pp. 1–16. https://doi.org/10.1016/j.isprsjprs.2020.11.015.

Tan, K., Thomas, G., Tong, R. and Li, J., 2015. Intensity data correction for the distance effect in terrestrial LASER scanners, *IEEE Journal of Selected Topics in Applied Earth Observations and Remote Sensing*, **9**(1), pp. 304–312. https://doi.org/10.1109/JSTARS.2015.2497310.

Yan, W.Y., Shaker, A., 2017. CORRECTION OF OVERLAPPING MULTISPECTRAL LIDAR INTENSITY DATA: POLYNOMIAL APPROXIMATION OF RANGE AND ANGLE EFFECTS. Int. Arch. Photogram. Remote Sens. Spatial Inf. Sci. XLII-3/W1, 177–182. https://doi.org/10.5194/isprs-archives-XLII-3-W1-177-2017